

## Prediction of intercluster separation and Schottky-type heat-capacity contribution in surface-segregated binary and ternary alloy nanocluster systems

Micha Polak and Leonid Rubinovich

Department of Chemistry, Ben-Gurion University of the Negev, Beer-Sheva 84105, Israel

(Received 27 October 2004; published 28 March 2005)

Site-specific average atomic concentrations computed for systems of Rh-Cu, Ni-Cu and Rh-Ni-Cu icosahedral and cuboctahedral free nanoclusters of different sizes by the “free-energy concentration expansion method” are used for evaluating pertinent cluster thermodynamic functions. Compared to stable surface segregated “magic-number” structures, at intermediate overall compositions the cluster system is expected to separate into these “phases.” A Schottky-type heat-capacity anomaly is predicted and attributed to atomic exchange (e.g., desegregation) excitation processes. Its measurement can elucidate the cluster segregation energetics.

DOI: 10.1103/PhysRevB.71.125426

PACS number(s): 61.46.+w, 68.35.Dv, 82.60.Qr

The growing interest in alloy nanocluster structure and property relationships has motivated the development of theoretical models, especially in view of limitations in current experimental tools. In particular, detailed knowledge of the cluster surface compositional patterns versus temperature, overall composition, shape, and size is essential for its optimal applicability in heterogeneous catalysis and other technologies based on highly dispersed particles. For such goals, several theoretical-computational approaches have been used with *ab initio* or many-body semiempirical energetics in conjunction with Monte Carlo computer simulations and molecular dynamics, as well as the genetic global optimization method.<sup>1,2</sup> Even simple pair-interaction energetics used in the Bragg-Williams (BW) approximation can furnish some insight into phenomena and properties specific to alloy clusters.<sup>3</sup> Most studies were focused on *single* binary clusters, while only few recent works studied cluster *systems*.<sup>4</sup>

The analytical free-energy concentration expansion method (FCEM), originally derived by us for the computation of equilibrium surface segregation in the presence of interatomic correlations (short-range order) in binary<sup>5-9</sup> and ternary<sup>10</sup> solid solutions, was recently adapted to multicomponent alloy clusters.<sup>11</sup> Being much more efficient compared to other methods, the FCEM can yield quite extensive amounts of data, facilitating systematic studies of complex cluster compositional structures for sizes reaching hundreds of atoms and more. Such data, covering wide ranges of temperature and compositions, form the basis for calculation of “cluster thermodynamic functions.”<sup>11</sup> In that first attempt to compute cluster compositional structures of a ternary alloy, intracluster separation via two-element competitive surface segregation with mixed or demixed order was predicted.<sup>11,12</sup>

This paper introduces two principal phenomena anticipated for alloy nanoclusters.

(a) Intercluster separation as a “phase transition.” Studies of this segregation-related equilibrium phenomenon are facilitated by applying the FCEM to a system of alloy clusters capable of exchanging constituent atoms<sup>11</sup> (irrespective of the kinetic mechanism of exchange).

(b) Schottky-type heat-capacity anomaly associated with the surface desegregation process. The computations show

that in contrast to bulk alloys, desegregation effects on the heat capacity of alloy nanoclusters are not negligible, but are comparable to the contribution of a classical degree of freedom ( $R/2$ ).

The FCEM is applied to perfect shape cuboctahedron (CO) and icosahedron (ICO) clusters consisting of 13–923 atoms distributed among concentric “shells.” This restriction of the cluster geometry to symmetric structures (ICO,CO) is a rather common assumption in cluster studies, which was confirmed experimentally<sup>13–16</sup> and by theoretical calculations [e.g., for Cu and Ni (Refs. 1, 17, and 18); low-symmetry, “amorphous” structures are expected for Au or Pt clusters,<sup>19,20</sup> but in general, amorphization tendencies decrease with increasing cluster size<sup>21</sup>].

The energetic parameters entering FCEM comprise the nearest-neighbor (NN) interaction energy  $w_{pq}^{IJ}$  based<sup>11,12</sup> on coordination-dependent site energies<sup>22</sup> and the effective interactions  $V_{pq}^{IJ}$  between constituents  $I$  and  $J$  [ $V_{pq}^{IJ} = 1/2(w_{pq}^{II} + w_{pq}^{JJ} - 2w_{pq}^{IJ})$ ]. Geometric input parameters include the number of atoms in each shell,  $N_p$ , and the number of NN pairs belonging to  $p$  and  $q$ -shells,  $N_{pq}$ .<sup>11</sup> Alloy free energy can be written<sup>6,7,11</sup> as the sum  $F = F^{BW} + \Delta F^{cor}$ , where  $F^{BW}$  is the BW-type contribution and  $\Delta F^{cor}$  is a correction related to interatomic correlations. In order to avoid exponential divergence at low temperatures in a case  $V_{pq}^{IJ} < 0$ , the FCEM formula for correlation functions<sup>10</sup> is approximated here by means of a product of hyperbolic tangent<sup>23</sup> and shell concentrations  $\varepsilon_{pq}^{IJ} = c_p^I c_p^J c_q^I c_q^J \tanh(b2V_{pq}^{IJ}/kT)$  [ $b=0.6$  from the best fit of FCEM predictions to Monte Carlo simulations of (100) surface segregation in fcc solid solution<sup>7</sup>]. Correspondingly, the revised correction term reads

$$\Delta F^{cor} = -kT \sum_{p \leq q} \left( N_{pq} \sum_{\{IJ\}} \left\{ c_p^I c_p^J c_q^I c_q^J \frac{1}{b} \times \ln \left[ \cosh \left( b \frac{2V_{pq}^{IJ}}{kT} \right) \right] \right\} \right).$$

Numerical minimization of  $F$  yields all  $I$ -constituent  $p$ -shell average concentrations ( $c_p^I$ ). The computations focus

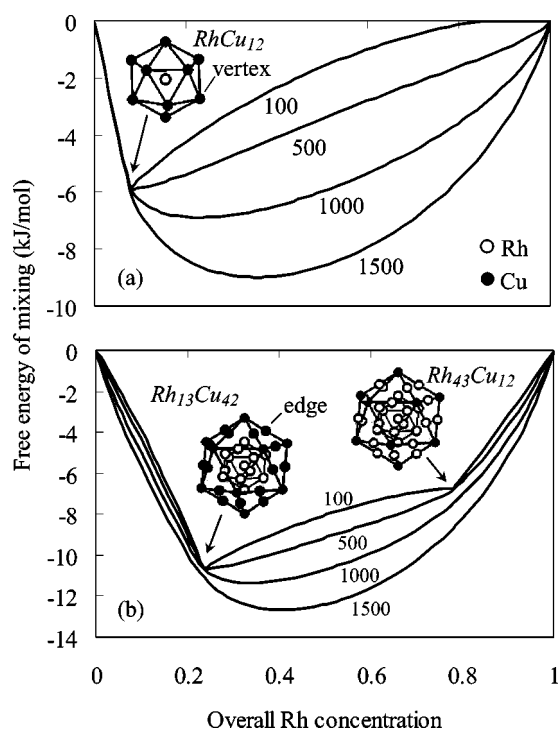


FIG. 1.  $F^{mix}$ - $c$  curves computed using FCEM output concentrations for Rh-Cu 2-shell 13-atom icosahedron (ICO) (a) and 4-shell 55-atom ICO clusters (b) at different temperatures (K). Convexity between the indicated magic-number compositions (structures) signifies intercluster separation.

mainly on the Rh-Cu cluster system characterized by moderately repulsive  $V^{Rh-Cu}$  [ $-23$  meV (Ref. 12)] and Cu site energies (and “surface energies”) much lower compared to Rh. Two additional systems reported here are Ni-Cu with lower repulsive  $V^{Ni-Cu}$  and smaller differences in site energies and Rh-Ni-Cu ternary clusters with all repulsive interactions. Cu segregation is expected for these systems, leaving behind a Rh or Ni rich core. Such a central-symmetric intracluster separation, amplified by the repulsive interactions, which differs principally from a nonsymmetric subcluster segregation,<sup>1,24</sup> is adequately characterized by shell concentrations.

**Magic numbers and cluster separation.** Some earlier attempts to evaluate segregation-separation phenomena in endothermic alloy clusters included Ni-Cu treated within the BW approximation<sup>3</sup> and Au-Ni using the pair approximation of the Kikuchi method.<sup>25</sup> The first study did not refer to intercluster separation, while the latter calculated “phase separation” lines for square and hexagonal 2D structures only. The FCEM applied to a system of three-dimensional (3D) polyhedron clusters is suitable for elucidation of intercluster separation coupled with intracluster surface segregation. Thus, the derived sets of shell concentrations can be considered as true equilibrium values only after inspecting the shape of the free-energy versus overall concentration curve. Figure 1(a) presents the mixing free energy of a Rh-Cu 13-atom ICO cluster, defined in Ref. 11 as the difference between the alloy and the pure element free energies. While the negative  $F^{mix}$  indicates no tendency for separation

into pure elemental clusters, at low temperatures it does reveal a region of convexity (i.e., a “miscibility gap”) between pure Rh and a marked minimum corresponding to a stable “magic” compositional structure,  $Rh_1Cu_{12}$ , having Rh at the center and Cu populating the surface vertexes. Hence, for intermediate overall compositions in the convex region, the system is unstable with respect to separation into  $Rh_1Cu_{12}$  and pure Rh clusters.

Larger clusters exhibit more diverse intercluster separation phenomena. Thus, for the 55-atom ICO structure two magic compositional structures are predicted. One,  $Rh_{13}Cu_{42}$ , with a Cu-segregated surface surrounding a Rh core, and in the other,  $Rh_{43}Cu_{12}$ , all edge sites are also Rh populated. In this case, the  $F^{mix}$ - $c$  curve shows at low temperatures two regions of convexity, one between pure Cu and the minimum at  $Rh_{13}Cu_{42}$ , and the other between  $Rh_{13}Cu_{42}$  and the break at  $Rh_{43}Cu_{12}$  [Fig. 1(b)]. Hence again, for overall intermediate compositions the clusters are unstable with respect to intercluster compositional separation involving these respective “phases.”

It should be emphasized that while bulk systems are characterized by phase transition points (e.g., melting, phase separation), transitions in a *single* small particle typically spread over a range of temperatures.<sup>26</sup> On the other hand, a *large system* of even the small ICO-13 clusters, which are capable of exchanging atoms, does exhibit an intercluster separation, characterized by a distinct transition temperature marked by the disappearance of the convexity (Fig. 1). In particular, the following transition temperatures were estimated: 580 K for  $Rh_1Cu_{12}/Rh_{13}$  separation and 440 K and 790 K for  $Rh_{13}Cu_{42}/Rh_{43}Cu_{12}$  and  $Cu_{55}/Rh_{13}Cu_{42}$  separations, respectively, all of which are lower than the bulk values [e.g.,  $\sim 1423$  K at  $\sim 60$  at % of Rh (Ref. 27)]. These results are in accordance with the depression of certain transition temperatures in small particles due to their reduced coordination.<sup>11,29</sup> Extending FCEM computations to ternary alloy clusters yielded for Rh-Ni-Cu 55-atom ICO the mixing free-energy versus overall concentration 3D plot shown in Fig. 2, which exhibits a global minimum at a “ternary magic composition,”  $Rh_{13}Ni_{30}Cu_{12}$  corresponding to core/edges/vertexes filled by Rh/Ni/Cu, respectively. A clear convexity region of intercluster separation involves the ternary and the previous two Rh-Cu magic compositions, and a somewhat weaker convexity is adjacent to the binary Ni-Cu line. To our best knowledge, these are the first computations of intercluster separation in ternary and binary alloy nanoclusters.

**Heat-capacity contributions.** The segregated, relatively stable “magic” compositional structures reveal thermal properties unique to alloy nanoclusters. The computed entropy shows distinct minima (Fig. 3, bottom) signifying these relatively ordered magic compositions, which gradually are weakened with increased temperature due to intracluster atomic site exchange. It can be noted that the  $Rh_{13}Cu_{42}$  structure is thermally more stable, as the entropy minimum still persists above 1100 K, while the other, corresponding to  $Rh_{43}Cu_{12}$ , already vanished. This marked difference is closely associated with excitation energies between differently coordinated atomic sites: surface to core Cu desegregation versus in-surface Cu (vertex)/Rh (edge) exchange in the latter structure. Such thermally induced processes (and cor-

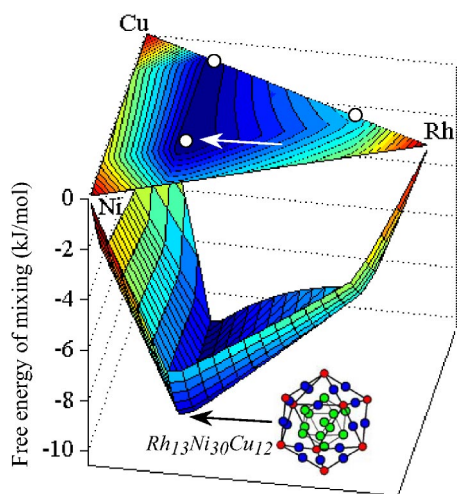


FIG. 2. Mixing free energy of ternary Rh-Ni-Cu 55-atom ICO cluster plotted with respect to the concentration Gibbs triangle (100 K). A major convexity region lies between circles on the 2D contour plot, marking magic compositions (arrows point at the  $F^{mix}$  global minimum computed for the “ternary magic composition”).

responding entropy variations) should contribute to the nanocluster heat capacity,  $C = \partial E / \partial T = T(\partial S / \partial T)$ . Indeed, the computed heat-capacity versus temperature “C -curves” (Fig. 3, top) exhibit a hump with a shape characteristic of a “Schottky anomaly,” originating from excitations between finite number of energy levels.<sup>28</sup> Only a few previous works mentioned similar effects on the cluster heat capacity, refer-

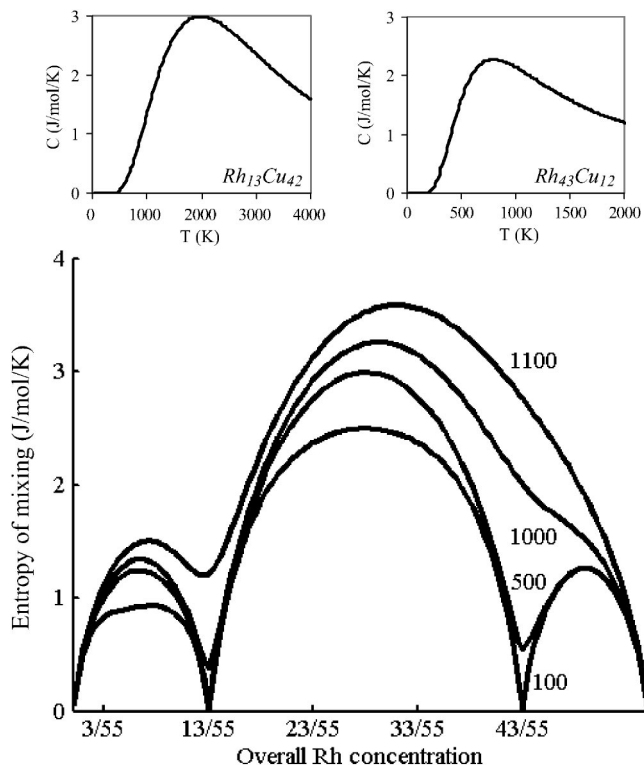


FIG. 3. S-c curves at different temperatures (K) computed for Rh-Cu 55-atom ICO clusters (bottom). Heat-capacity curves corresponding to the two magic compositions (top).

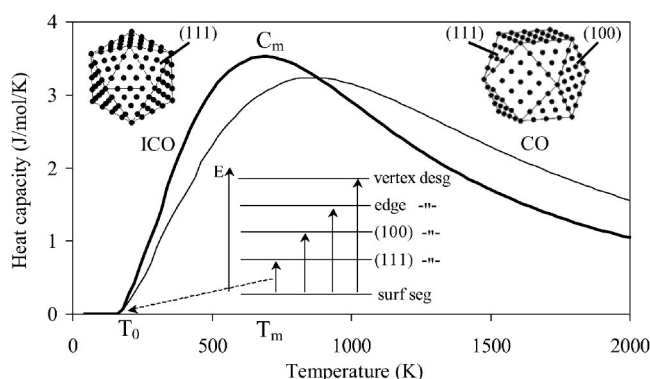


FIG. 4. Schottky-type desegregation contribution to the cluster heat capacity: 309-atom ICO vs CO clusters having Ni<sub>147</sub>Cu<sub>162</sub> “magic” composition. The lowest level in the energy scheme corresponds to a completely Cu surface-segregated cluster, and desegregation excitations of single Cu atom to the Ni core are indicated by vertical arrows.  $T_0$  signifies the onset of the desegregation effect involving the lowest (111) excitation.  $T_m$  and  $C_m$  refer to the heat-capacity maximum.

ring to “order-disorder transitions” in Pd<sub>7</sub>Ni<sub>6</sub> clusters<sup>24</sup> and to “isomerization structural transitions” in bimetallic Cu-Ni cubic nanoclusters.<sup>29</sup> While exploring systematically effects of cluster size, shape and energetics, the present work identified the heat capacity Schottky-type behavior, attributed to gradual desegregation (or atomic exchange) excitation processes.

Figure 4 displays C curves of ICO-309 compared to CO-309 together with energy level scheme illustrating pertinent excitations. The lowest excitation energy involves in both structures Cu desegregation from the fully segregated (111) face to the core, thus yielding the same  $T_0$  value [the absence of (111) faces in 13- and 55-atom clusters leads to somewhat higher  $T_0$  values]. Unlike  $T_0$ ,  $T_m$  depends not only on the lowest excitation energy of the (111)-core exchange, but on the whole spectrum of excitation energies from faces, edges, and vertexes, and therefore should be related to some average surface coordination. The  $\sim 170$  K higher  $T_m$  of the CO is attributed to its relatively more open surface (see Fig. 4) and correspondingly higher average excitation energy. Desegregation (segregation) energies are roughly proportional to the difference of constituent surface energies. Indeed, a ratio  $T_0(\text{Rh-Cu})/T_0(\text{Ni-Cu}) \approx 3.2$  computed for various size CO clusters is comparable to the (111) surface energy difference ratio estimated for these systems,  $\sim 3.9$ . Moreover, the computed ratio  $T_m(\text{Rh-Cu})/T_m(\text{Ni-Cu}) \approx 2.7$  falls between the ratio  $\sim 2.8$  for (100) faces and  $\sim 2.5$  for edges. Similarly, the almost twice larger  $T_m$  and  $T_0$  values obtained for Rh<sub>13</sub>Cu<sub>43</sub> compared to Rh<sub>43</sub>Cu<sub>12</sub> (Fig. 3) are closely associated with the different coordination-dependent excitation energies mentioned above. Generally, for  $T > T_m$  (which might not be always experimentally accessible) C decreases due to gradually diminished desegregation until all atoms are randomly distributed over all cluster sites (complete mixing).

The heat-capacity characteristic magnitude ( $C_m$ ) is expected to correlate with the number of all surface-core desegregation excitations that randomize the initial fully segregated cluster. The number of these excited configurations is

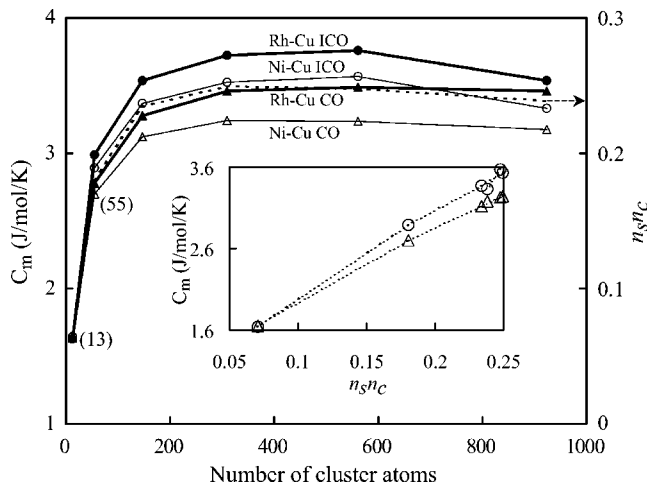


FIG. 5. The maximum heat capacity computed for 13 to 923-atom ICO and CO Rh-Cu and Ni-Cu clusters with overall magic compositions (Cu surface, Rh or Ni cores). Dashed line: the product of surface and core site fractions, representing the number of surface-core desegregation excitations. Inset:  $C_m$  of Ni-Cu ICO and CO clusters plotted as a function of the fraction product.

proportional to the product of the surface and core site fractions,  $n_s n_c$ . This anticipated trend is confirmed by the computed  $C_m$  that reaches a maximum for 561 atom clusters (Fig. 5) following the same pattern as the  $n_s n_c$  product and exhibiting linear dependence for a given alloy and cluster shape (Fig. 5, inset). Furthermore, in accordance with analysis of Schottky anomaly in a simple two-level system,<sup>28</sup>  $C_m$  is expected to increase with the respective degeneracy of excited energy levels in equal  $n_s n_c$  and size ICO and CO clusters. Indeed,  $C_m$  is somewhat higher for the ICO clusters (Fig. 5, also see Fig. 4), having more uniform surface and hence more degenerated excited levels compared to CO clusters. This shape-related degeneracy factor seems to affect  $C_m$  more than does the chemical identity of constituents (Fig. 5). The two-level model<sup>28</sup> with degeneracy ratio 12 pertinent to the 13-atom clusters, having a single solute atom either at the center or at the surface [see Fig. 1(a)] predicts for both ICO and CO  $C_m = 1.55$  J/mol/k, in good agreement with the present calculations (Fig. 5). Further computations for the two binary alloy clusters with sizes up to 923 atoms confirm the universality of the  $C$  curves as a Schottky-type anomaly, which is notably evident when reduced coordinates  $T/T_m$  and  $C/C_m$  are used.<sup>33</sup> Similar heat-capacity behavior was revealed in computations for clusters with a ternary magic composition—e.g., the above-mentioned  $\text{Rh}_{13}\text{Ni}_{30}\text{Cu}_{12}$  ICO's. In this case, since at low temperatures Ni/Cu edge-vertex exchange dominates and at higher temperatures atomic exchange occurs mainly between the Rh core and Ni-rich mixed Ni-Cu surface, the computed ternary  $C$  curve is nearly a superposition of the binary  $\text{Rh}_{13}\text{Ni}_{42}$  and  $\text{Ni}_{43}\text{Cu}_{12}$  contributions.

In conclusion, the particular statistical-mechanical frame-

work chosen, involving a system of atom exchanging clusters and the remarkable efficiency of the FCEM (compared to *ab initio* or semiempirical-based simulations) in computing nanocluster compositional structures and related thermodynamical functions, enabled us to reveal two noteworthy phenomena: intercluster separation coupled with intracluster surface segregation at “magic number” compositions and Schottky-type heat-capacity anomaly, mentioned and analyzed for the first time in the context of desegregated clusters. It should be noted that both phenomena are thermodynamically valid, irrespective of the energetic model or method used to compute cluster compositional structures (e.g., the shape of the heat-capacity curve). On the other hand, the accuracy of the computational results depends to a large extent on the particular energetic model and parameters chosen. Clearly, cluster-structure *ab initio* quantum-mechanical calculations [e.g., based on density function theory (DFT)] are highly desirable. However, they are presently, feasible only for very small clusters.<sup>2,15</sup> For larger clusters computer simulations with semiempirical many-body potentials (embedded atom method or tight-binding second-moment approximation) have been used, in spite of problems related to diminished surface energies<sup>30</sup> or overestimated cohesion energy<sup>31</sup> (most recently, an attempt to improve parametrization of the potentials for modeling low coordination interactions was reported<sup>32</sup>). In the present case of medium- or large-size *multicomponent* alloy clusters, in spite of its limitations, the FCEM with coordination-dependent site energies, based on experimental cohesion and surface energies, appears to be a practical reasonable approach. While measurements of site-specific compositions in a nanocluster are well beyond the capabilities of current experimental tools, the situation with the two predicted thermodynamic phenomena seems to be more promising. In particular, mass spectrometric experiments are expected to detect coexisting stable magic-composition clusters. Furthermore, as shown above, for all studied cluster sizes the Schottky anomaly is not negligible ( $\sim R/2$ ) and is expected to be detected experimentally. In a recent elaborate experiment, the heat capacity of free Na nanoclusters were determined from the temperature dependence of the photofragmentation mass spectrum.<sup>26</sup> In case such experiments could be extended to alloy nanoclusters, heat-capacity measurements ( $T_0, T_m$ ) would elucidate the alloy cluster segregation energetics. ( $C_m$  may furnish some indications regarding the cluster size.) However, such estimations are limited to alloy systems for which the thermal excitations contributing to the heat capacity occur at temperatures sufficiently different from surface or bulk melting temperatures. This can include cases of weak (core to surface) segregation in general or in-surface processes such as the low-energy Cu (vertex)/ Rh (edge) exchange (Fig. 3, top-right). These and further theoretical<sup>33</sup> (and experimental) studies of cluster thermodynamics are expected to shed light on useful properties of alloy nanocluster systems.

- <sup>1</sup>L. Johnston, J. Chem. Soc. Dalton Trans. **22**, 4193 (2003).
- <sup>2</sup>F. Baletto and R. Ferrando, Rev. Mod. Phys. (to be published).
- <sup>3</sup>J. M. Montejano-Carrizales and J. L. Moran-Lopez, Surf. Sci. **239**, 169 (1990); **239**, 178 (1990).
- <sup>4</sup>M. Hou, V. S. Kharlamov, and E. E. Zhurkin, Phys. Rev. B **66**, 195408 (2002).
- <sup>5</sup>M. Polak, J. Deng, and L. Rubinovich, Phys. Rev. Lett. **78**, 1058 (1997).
- <sup>6</sup>M. Polak and L. Rubinovich, Surf. Sci. Rep. **38**, 127 (2000).
- <sup>7</sup>J. M. Roussel, A. Saul, L. Rubinovich, and M. Polak, J. Phys.: Condens. Matter **11**, 9901 (1999).
- <sup>8</sup>M. Polak and L. Rubinovich, in *Alloy Surface Segregation and Ordering Phenomena: Recent Progress*, edited by D. P. Woodruff, Surface Alloys and Alloy Surfaces, The Chemical Physics of Solid Surfaces, Vol. 10 (Elsevier Science, Amsterdam, 2002).
- <sup>9</sup>M. Polak, C. S. Fadley, and L. Rubinovich, Phys. Rev. B **65**, 205404 (2002).
- <sup>10</sup>L. Rubinovich and M. Polak, Surf. Sci. **513/1**, 119 (2002).
- <sup>11</sup>L. Rubinovich and M. Polak, Phys. Rev. B **69**, 155405 (2004).
- <sup>12</sup>M. Polak and L. Rubinovich, Int. J. Nanosci. **3**, 625 (2004).
- <sup>13</sup>M. Pellarin, B. Baguenard, J. L. Vialle, J. Lerme, M. Broyer, J. Miller, and A. Perez, Chem. Phys. Lett. **217**, 349 (1994).
- <sup>14</sup>D. Reinhard, B. D. Hall, P. Berthoud, S. Valkealahti, and R. Monot, Phys. Rev. Lett. **79**, 1459 (1997).
- <sup>15</sup>J. A. Alonso, Chem. Rev. (Washington, D.C.) **100**, 637 (2000).
- <sup>16</sup>Zu Rong Dai, Shouheng Sun, and Zhong L. Wang, Surf. Sci. **505**, 325 (2002).
- <sup>17</sup>F. Baletto, R. Ferrando, A. Fortunelli, F. Montalenti, and C. Mottet, J. Chem. Phys. **116**, 3856 (2002).
- <sup>18</sup>C. Massen, T. V. Mortimer-Jones, and R. L. Johnston, J. Chem. Soc. Dalton Trans. **23**, 4375 (2002).
- <sup>19</sup>I. L. Garzon, K. Michaelian, M. R. Beltran, A. Posada-Amarillas, P. Ordejon, E. Artacho, D. Sanchez-Portal, and J. M. Soler, Phys. Rev. Lett. **81**, 1600 (1998).
- <sup>20</sup>E. Apra, F. Baletto, R. Ferrando, and A. Fortunelli, Phys. Rev. Lett. **93**, 065502 (2004).
- <sup>21</sup>J. M. Soler, M. R. Beltran, K. Michaelian, I. L. Garzon, P. Ordejon, D. Sanchez-Portal, and E. Artacho, Phys. Rev. B **61**, 5771 (2000).
- <sup>22</sup>Ling Zhu and A. E. De Pristo, J. Catal. **167**, 400 (1997).
- <sup>23</sup>In the Ising model hyperbolic tangent appears in pair correlation functions and is used as expansion parameter, e.g., J. M. Ziman, *Models of Disorder: The Theoretical Physics of Homogeneously Disordered Systems* (Cambridge University Press, Cambridge, England, 1979). The hyperbolic tangent closely reproduces FCEM correlation functions in the case  $V_{pq}^{IJ} > 0$ .
- <sup>24</sup>M. C. Vicens and G. E. Lopez, Phys. Rev. A **62**, 033203 (2000).
- <sup>25</sup>J. L. Moran-Lopez and L. M. Falicov, in *Alloy Phase Diagrams*, edited by L. H. Bennett, T. B. Massalski, and B. C. Eiesian, MRS Symposia Proceedings No. 19 (Materials Research Society, Pittsburgh, 1983), p. 29.
- <sup>26</sup>M. Schmidt, R. Kusche, W. Kronmuller, B. von von, and H. Haberland, Phys. Rev. Lett. **79**, 99 (1997); M. Schmidt and H. Haberland, C. R. Phys. **3**, 327 (2002).
- <sup>27</sup>*Binary Alloy Phase Diagrams*, edited by T. B. Massalski, H. Okamoto, P. R. Subramanian, and L. Kacprzak (ASM International, Materials Park, OH, 1990).
- <sup>28</sup>E. S. R. Gopal, *Specific Heats at Low Temperatures* (Plenum Press, New York, 1966).
- <sup>29</sup>Shi-Ping Huang and P. B. Balbuena, J. Phys. Chem. B **106**, 7225 (2002).
- <sup>30</sup>V. Rosato, M. Guillope, and B. Legrand, Philos. Mag. A **59**, 321 (1989).
- <sup>31</sup>C. Mottet, G. Treglia, and B. Legrand, Phys. Rev. B **66**, 045413 (2002).
- <sup>32</sup>T. Van Hoof and Marc Hou, Appl. Surf. Sci. **226**, 94 (2004).
- <sup>33</sup>M. Polak and L. Rubinovich, Surf. Sci. (in press).